JOURNAL OF BACTERIOLOGY, July 1997, p. 4143–4157 Vol. 179, No. 13
0021-9193/97/$04.00+0

Aspartate Transcarbamylase from the Deep-Sea Hyperthermophilic Archaeon *Pyrococcus abyssi*: Genetic Organization, Structure, and Expression in *Escherichia coli*

CRISTINA PURCAREA,[1,2] GUY HERVÉ,[2] MONCEF M. LADJIMI,[3] AND RAYMOND CUNIN[1]*

Laboratorium voor Erfelijkheidsleer en Microbiologie, Instituut voor Moleculaire Biologie en Biotechnologie, Vrije Universiteit Brussel en Vlaams Interuniversitair Instituut voor Biotechnologie, 1070 Brussels, Belgium,[1] and Laboratoire de Biochimie des Signaux Régulateurs Cellulaires et Moléculaires, URA CNRS 1682—Université Pierre et Marie Curie, 75006 Paris,[2] and Laboratoire d'Enzymologie et Biochimie Structurales, CNRS, 91190 Gif-sur-Yvette,[3] France

Received 8 November 1996/Accepted 19 March 1997

The genes coding for aspartate transcarbamylase (ATCase) in the deep-sea hyperthermophilic archaeon *Pyrococcus abyssi* were cloned by complementation of a *pyrB Escherichia coli* mutant. The sequence revealed the existence of a *pyrBI* operon, coding for a catalytic chain and a regulatory chain, as in *Enterobacteriaceae*. Comparison of primary sequences of the polypeptides encoded by the *pyrB* and *pyrI* genes with those of homologous eubacterial and eukaryotic chains showed a high degree of conservation of the residues which in *E. coli* ATCase are involved in catalysis and allosteric regulation. The regulatory chain shows more-extensive divergence with respect to that of *E. coli* and other *Enterobacteriaceae* than the catalytic chain. Several substitutions suggest the existence in *P. abyssi* ATCase of additional hydrophobic interactions and ionic bonds which are probably involved in protein stabilization at high temperatures. The catalytic chain presents a secondary structure similar to that of the *E. coli* enzyme. Modeling of the tridimensional structure of this chain provides a folding close to that of the *E. coli* protein in spite of several significant differences. Conservation of numerous pairs of residues involved in the interfaces between different chains or subunits in *E. coli* ATCase suggests that the *P. abyssi* enzyme has a quaternary structure similar to that of the *E. coli* enzyme. *P. abyssi* ATCase expressed in transgenic *E. coli* cells exhibited reduced cooperativity for aspartate binding and sensitivity to allosteric effectors, as well as a decreased thermostability and barostability, suggesting that in *P. abyssi* cells this enzyme is further stabilized through its association with other cellular components.

Studies of extremophilic organisms provide information on the molecular mechanisms of biological adaptation to extreme environments. In this regard, *Pyrococcus abyssi* is of particular interest, being a hyperthermophilic and barophilic/barotolerant archaeon. This euryarchaebacterium, isolated from a deep-sea hydrothermal vent located 2,000 m deep in the North Fiji Basin, was characterized by Erauso et al. (15, 16). It is a heterotrophic and strictly anaerobic microorganism and belongs to the sulfur-metabolizing group. At atmospheric pressure, it grows at 67 to 102°C, with an optimum at 96°C. Hydrostatic pressure slightly increases the growth rate of *P. abyssi* as well as its optimal and maximal growth temperatures (16).

Aspartate transcarbamylase (ATCase) (EC 2.1.3.2) is the first enzyme of the pyrimidine biosynthetic pathway. It catalyzes the carbamylation of the amino group of aspartate by carbamylphosphate with formation of carbamylaspartate and phosphate. ATCase is extensively studied as a model for structure-function relationships in cooperativity and allosteric regulation mechanisms, as well as for the evolution of these mechanisms from prokaryotes to humans. The structure and properties of the *Escherichia coli* enzyme have been studied in detail (for reviews, see references 3, 10, 26, 32, 40, and 70). This dodecameric enzyme (78) is composed of two types of polypeptide chains: the catalytic chains (c) encoded by the *pyrB* gene (30) and regulatory chains (r) encoded by the *pyrI* gene (66). The quaternary structure of this enzyme results from the association of two catalytic c3 subunits (trimers of catalytic chains of 310 amino acids; molecular weight, 34,301) held together through their interactions with three regulatory r2 subunits (dimers of regulatory chains of 152 amino acids; molecular weight, 17,109) (8). Both types of chains are organized in two domains, the carbamylphosphate and the aspartate binding domains in the case of the catalytic chain and the allosteric and the zinc (Zn) domains in the case of the regulatory chain. The regulatory chain contains a zinc atom coordinated to four cysteine residues clustered near its C terminus (24). The presence of this cation ensures the proper folding of the domain for its interactions with the catalytic subunits. The catalytic sites are located at the interface between two catalytic chains belonging to the same trimer and involve residues belonging to both chains (36, 44). These structural features were found in homologous enterobacterial enzymes. It is noteworthy that, so far, it is only in these microorganisms that ATCase comprises regulatory chains (77).

E. coli ATCase shows cooperativity for the binding of its substrate aspartate, a phenomenon which is explained by the transition from a T state having a low affinity for aspartate to an R state which has a high affinity for this substrate. The crystallographic structures of these two extreme conformations are known with a resolution of 2.5 Å (28, 29, 33, 35, 36). In the

* Corresponding author. Mailing address: Laboratorium voor Erfelijkheidsleer en Microbiologie, Instituut voor Moleculaire Biologie en Biotechnologie, Vrije Universiteit Brussel en Vlaams Interuniversitair Instituut voor Biotechnologie, 1, E. Grysonlaan, 1070 Brussels, Belgium.

R state, the two catalytic subunits are no longer in close contact. *E. coli* ATCase is also subject to allosteric regulation. Its activity is synergistically feedback inhibited by the two end products CTP and UTP and is stimulated by ATP. These effectors bind to the same regulatory sites, at a distance of 60 Å from the catalytic sites (28). Interfaces between the subunits and between the domains of both chains play important roles in these regulatory properties (9, 12, 23, 33).

ATCases from other eubacterial and eukaryotic organisms are composed either of only catalytic chains, as in *Bacillus subtilis* (39) and *Lycopersicum esculentum* (54), or of catalytic chains associated with other enzymes of the pyrimidine pathway, as in *Pseudomonas putida* (67), *Saccharomyces cerevisiae* and *Schizosaccharomyces pombe* (41, 69), or mammals (10, 17, 68).

The enzymatic properties of several ATCases from extremophiles, including the halophilic archaeon *Halobacterium cutirubrum* (52), the halophilic eubacterium *Vibrio costicola* (1), and the (hyper)thermophilic eubacteria *Thermotoga maritima* and *Thermus aquaticus* (74), were previously investigated. These enzymes exhibit differences in their regulatory properties.

Recently, the determination of the entire genomic sequence of the archaeon *Methanococcus jannaschii* (6) revealed the existence of two open reading frames (ORFs) potentially coding for the ATCase catalytic chain (*pyrB*) and for a regulatory chain (*pyrI*). These genes are separated on the chromosome.

A particularity of the ATCase reaction in thermophilic and hyperthermophilic organisms is related to the high thermolability of one of its substrates, carbamylphosphate (2, 75), whose decomposition produces cyanate, a toxic, indiscriminate carbamylating agent (37).

The catalytic and regulatory properties of *P. abyssi* ATCase (strain GE5) were investigated previously (58, 59). This enzyme shows apparent cooperativity for both substrates. It is subject to allosteric regulation. At 37°C, it is feedback inhibited by both CTP and UTP and activated by ATP, although at high temperatures only the CTP effect is observed. *P. abyssi* ATCase is extremely stable at high temperatures and pressures. The purification of this enzyme led to alterations of its cooperative and allosteric properties, suggesting that in *P. abyssi*, the ATCase is stabilized by association with another cellular component (59).

In the present work, the *P. abyssi* gene coding for ATCase was cloned and expressed in *E. coli*. Sequencing showed the existence of two genes coding for a catalytic chain and a regulatory chain. The deduced primary structures were analyzed in comparison with those of homologous enzymes, and modeling was used for a more detailed comparison with the *E. coli* protein. The properties of the enzyme produced in *E. coli* (regulation, thermostability, and barostability) are partially altered relative to those of the enzyme in its native host.

MATERIALS AND METHODS

Chemicals, enzymes, and DNA molecular weight markers. Nucleotides were purchased from Sigma Chemical Co.; Tris-base was from Prolabo; 2-mercaptoethanol was from Kodak; [U-^{14}C]aspartate (300 mCi mmol^{-1}; 11.1 GBq mmol-1) was from CEA-Saclay; and restriction enzymes and DNA molecular weight marker III were from Boehringer Mannheim. TBE buffer used for the cell extracts contains 50 mM Tris HCl (pH 8), 1 mM 2-mercaptoethanol, and 0.1 mM EDTA.

Bacterial strains. *P. abyssi* GE5 was described by Erauso et al. (16). The following *E. coli* strains were used: XL1-Blue MRF′ {Δ(*mcr*A)183 Δ(*mcrCB-hsdSMR-mrr*) 173 *endA1 supE44 thi-1 recA1 gyrA96 relA1 lac*/F′ [*proAB lacI*^{q}*Z*Δ*M15* Tn*10*(Tet^r)]} (Stratagene); JM103*pyrB*$^-$ {Δ*lac-pro supE thi strA endA sbcB15 hsdR4*/F′ [*traD36 proAB lacI*^{q}*Z*Δ*M15* Δ*pyrB*]}, which is a *pyrB* derivative of JM103 (45) obtained from J. Wild (Texas A&M University); and EK1104 (F$^-$ *ara thi* Δ*pro-lac* Δ*pyrB pyrF*$^{\pm}$ *rpsL*) (53).

Growth media. The GE5 strain of *P. abyssi* was grown anaerobically on an enriched marine mineral medium containing cysteine as a sulfur source (16). The transgenic *E. coli* cells were grown either on 853 broth (22) or on 132 minimal mineral medium (22), supplemented with 0.5% glucose, 0.0001% thiamine, 0.005% proline, and 50 μg of kanamycin per ml or 100 μg of ampicillin per ml.

Vectors. Lambda ZAP Express vector previously restricted with *Bam*HI, pBK-CMV (Stratagene), and Bluescript II KS$^+$ (Stratagene) were used as vectors.

Chromosomal DNA preparation. The extraction and purification of *P. abyssi* chromosomal DNA were performed by using a CsCl gradient, as described previously (7).

Library construction. A *P. abyssi* genomic library was constructed by using the predigested ZAP Express *Bam*HI/CIAP cloning system (Stratagene). *P. abyssi* chromosomal DNA (40 μg) was partially digested with *Sau*3A (7.5 U) for 5, 10, 15, and 20 min at room temperature. Two 5-μg samples of this DNA digest were each ligated with 1 μg of *Bam*HI-predigested Lambda ZAP Express vector by incubation for 16 h at 16°C in the presence of 1 mM ATP, with 2 U of T4 ligase in final volumes of 5 and 20 μl. Packaging and amplification were performed as specified by Stratagene. The titer of the library was 10^{10} PFU/ml.

In vivo excision of pBK-CMV phagemids and selection of *pyrB*-complementing clones. Helper phage-mediated excision was performed by coinfecting 200 μl of XL1-Blue MRF′ cells (grown to an optical density at 600 nm [OD_{600}] of 0.3 and resuspended in 10 mM $MgSO_4$ at an OD_{600} of 5.0) with 2.5×10^9 PFU of the Lambda ZAP library and 10^8 PFU of ExAssist helper phage (Stratagene). The excised phagemids were used immediately to infect 600 μl of JM103*pyrB*$^-$ cells (OD_{600} = 0.5), and the cells were plated on appropriately supplemented minimal medium for complementation screening (80).

Southern hybridization. Southern hybridization was performed at 70°C, using random-primed probe labeling and hybridization conditions specified for the DIG labeling and detection system (Boehringer Mannheim).

Sequencing. Nucleotide sequencing was performed by the dideoxy chain termination method (65) in both directions with two universal primers. Overlapping clones were produced by exonuclease III (Exo III) partial digestion (25). Deletions were generated from *Kpn*I/*Eco*RI and *Bst*XI/*Xba*I double restrictions.

Enzymatic tests. ATCase activity was measured as described previously (57). Samples of dialyzed cell extracts were incubated at 37°C for 10 min in the presence of 20 mM aspartate, 5 mM carbamylphosphate, and 50 mM Tris HCl, pH 8. The ATCase activity of these extracts was defined as units per milligram of proteins, where a unit is the amount of enzyme which synthesizes 1 μmol of carbamylaspartate per h.

The nucleotide solutions were adjusted to pH 8, and the ATCase activity was measured as described above but in the presence of 3 mM aspartate. Percent activation was calculated as follows: % activation = $(V_a - V_0/V_0) \times 100$, where V_a is the reaction rate in the presence of allosteric effector and V_0 is the reaction rate in its absence.

Hydrostatic-pressure assays. The influence of hydrostatic pressure on the stability of ATCase was determined by using a previously described high-pressure reactor (31) which allows injection, mixing, and sampling without release of pressure.

Sequence alignments and structural modeling. Sequence comparison was performed by using the GAP program from the Genetics Computer Group 8.1 software package (49). Secondary structure was predicted by using the PHDsec program from the PredictProtein server (61–63), and multiple alignments were performed by using the MaxHom.SSP program from the same server (64). The Hydrophobic Cluster Analysis (HCA) program was used for analysis of hydrophobic clusters (20, 38). Modeling of the tridimensional structure was performed by amino acid replacement and energy minimization with the Swiss-Model program of the ExPaSy server (55, 56) and the Insight II and Homology programs (Biosym Technologies Co.).

Nucleotide sequence accession number. The nucleotide and amino acid sequences of the insert of the pAT3 clone containing the *P. abyssi pyrBI* operon were assigned accession no. U61765.

RESULTS

Construction of a genomic library of *P. abyssi*. A genomic library of the GE5 strain of *P. abyssi* was obtained by ligating *P. abyssi* chromosomal DNA partially digested with *Sau*3A in the Lambda ZAP Express vector previously restricted with *Bam*HI. The titer of the library was 10^{10} PFU/ml. The sizes of the inserts ranged from 1 to 12 kb.

Molecular cloning in *E. coli* and identification of the *pyrB* and *pyrI* genes from *P. abyssi*. The gene coding for the ATCase in *P. abyssi* was cloned by screening the genomic library for complementation of a *pyrB*-deficient derivative of *E. coli* JM103. After in vivo excision of pBK-CMV phagemids containing inserts of *P. abyssi* DNA, JM103*pyrB*$^-$ cells were infected at a multiplicity of infection of 50 (80). Fourteen colonies were obtained after 2 days of incubation on plates of

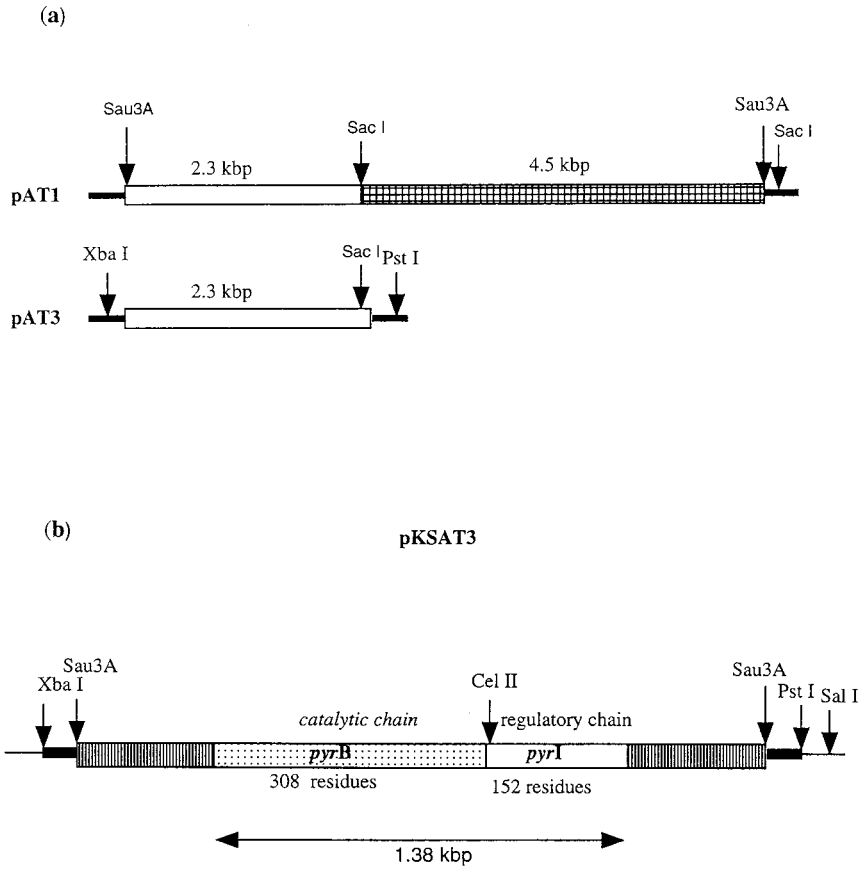

FIG. 1. Clones of ATCase genes from *P. abyssi*. (a) pAT1 and pAT3 clones in the pBK-CMV vector. Vector DNA (thick black lines) is indicated. (b) The pKSAT3 clone containing the *pyrB* and *pyrI* genes flanked by *P. abyssi* DNA (shaded segments). DNAs from the pBK-CMV vector and the Bluescript II KS$^+$ vector (thick black lines and thin lines, respectively) are indicated.

minimum medium supplemented with Casamino Acids and kanamycin. The thermal stability of the ATCase activity in cell extracts prepared from cultures of each of these candidates was investigated. It was found that after 10 min of incubation at 90°C, the activity was conserved up to 53 to 75%. Under similar conditions, *E. coli* ATCase was fully inactivated. This indicated that these clones code for a thermostable ATCase expressed in the *E. coli* host.

Two types of clones were obtained, differing by the size of the inserts: pAT1, with an insert of 6.8 kbp, and pAT3, with an insert of 2.3 kbp (Fig. 1a). A restriction analysis of these clones showed that pAT1 contains an additional *Sac*I fragment of 4.5 kbp situated downstream relative to the ATCase sequence present in pAT3.

The insert of pAT3 was recloned as a 2.3-kbp *Xba*I/*Pst*I fragment into the Bluescript II KS$^+$ vector. The resulting construction was designated pKSAT3 (Fig. 1b). The *P. abyssi* origin of the pKSAT3 insert was verified by Southern hybridization.

Sequence of the *P. abyssi* ATCase gene. The sequence of the *P. abyssi* DNA insert contains a 924-bp ORF coding for a protein of 308 residues (calculated molecular mass, 34,879 Da) homologous to the catalytic chain of *E. coli* ATCase (Fig. 2). This ORF was therefore designated *pyrB*. It is followed by a 456-bp ORF homologous to the *pyrI* gene of *Enterobacteriaceae*, which codes for the regulatory chain of ATCase from these microorganisms, and corresponding to a protein of 152 residues (calculated molecular mass, 16,947 Da). A particular feature of this archaeal *pyrBI* gene cluster is the absence of an intercistronic sequence between *pyrB* and *pyrI*, in contrast with all homologous enterobacterial operons.

In the pKSAT3 clone, the *pyrBI* gene cluster is flanked by 434 nucleotides upstream and 507 nucleotides downstream of it. The upstream region contains the C-terminal portion of a 377-bp ORF corresponding to 125 amino acids (Fig. 2), homologous to carbamylphosphate synthetases (CPSases). The region downstream from *pyrBI* contains the N-terminal region (67 residues) of an ORF which presents similarity with *E. coli* lipopolysaccharide heptosyltransferase 1.

Expression of the *P. abyssi* ATCase genes in *E. coli*. Complementation of the ATCase deficiency of *E. coli* cells by the corresponding genes from *P. abyssi* shows that these genes are expressed in a mesophilic eubacterial host. In rich medium containing uracil, the ATCase activity of cell extracts of the transgenic *E. coli* is 15 U · mg^{-1} of total protein, compared to 2.5 U · mg^{-1} in *P. abyssi* cell extracts. In minimal medium, the expression of the cloned genes is insensitive to added uracil at concentrations ranging from 4 to 50 mg · ml^{-1}, which suggests that in *E. coli*, it is not regulated by uracil.

Codon usage in the *P. abyssi pyrB* and *pyrI* genes. Codon usage in the archaeal *pyrB* and *pyrI* genes is significantly different from that observed in the homologous *E. coli* genes (30, 66). In particular, codons ATA (Ile), AAG (Lys), GAG (Glu), and AGG (Arg) are frequently used in the archaeal genes, while they are rarely used or even absent (AGG) in the *E. coli* *pyrBI* operon (a quantitative comparison is available on re-

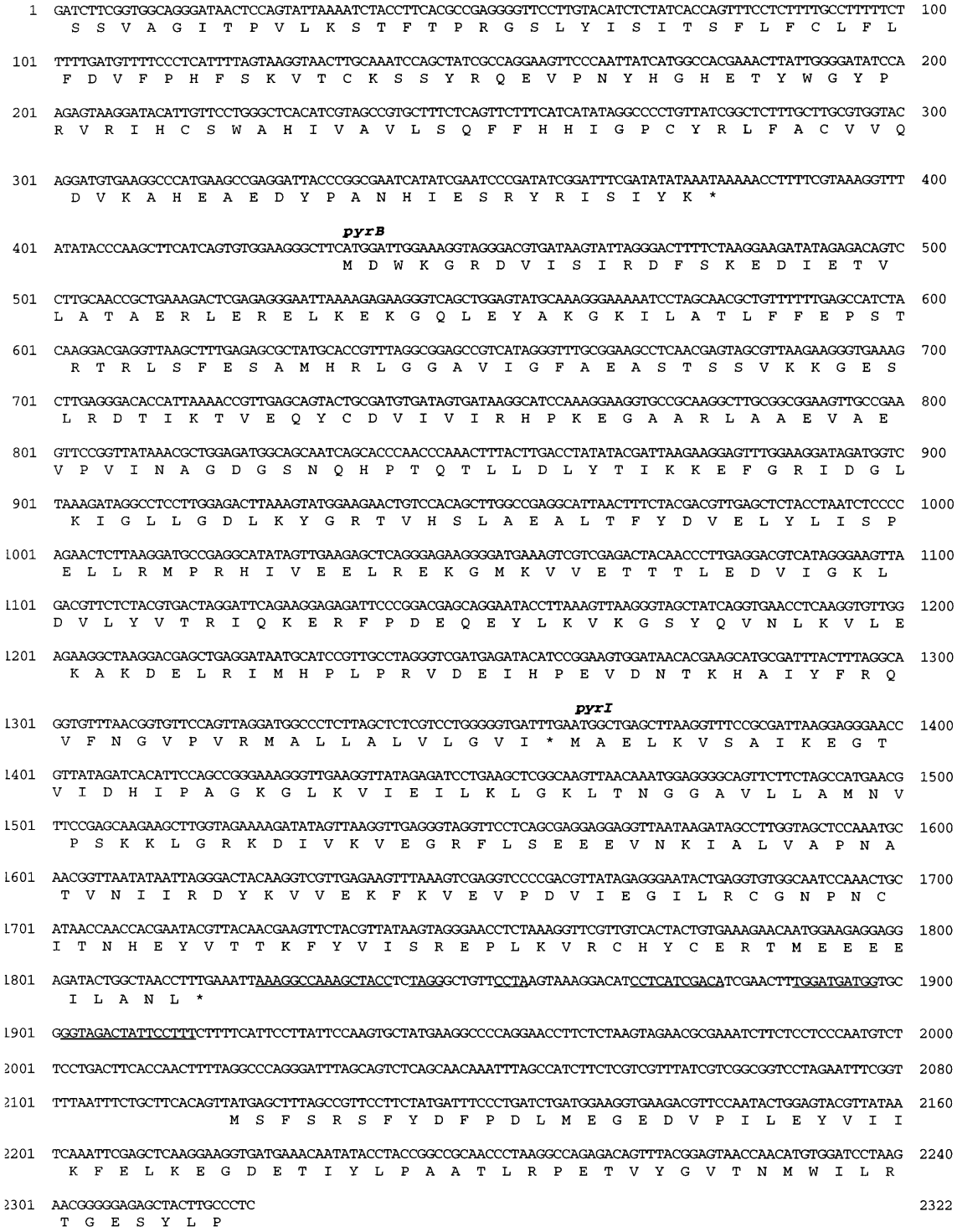

FIG. 2. Nucleotide sequence of the insert of pKSAT3 containing the *P. abyssi pyrBI* operon. The deduced amino acid sequences of PyrB and PyrI polypeptides are shown below the DNA sequence. Also shown are the products of two flanking coding regions. Amino acids are indicated by the one-letter code.

quest). This bias could present a problem for the overexpression of these *P. abyssi* genes in *E. coli* cells.

A characteristic of *Archaea* is a higher frequency of RNY codons (R = purine, Y = pyrimidine, N = purine or pyrimidine) and G/non-G/N codons in the coding reading frame than in the +1 and +2 frames (5). This is also the case in the *P. abyssi pyrB* and *pyrI* genes.

Functional analysis of the *pyrI*-encoded protein. In order to investigate the role of the polypeptide coded by *pyrI* in *P. abyssi*, a 1.01-kbp *Cel*II-*Sal*I fragment was removed from the

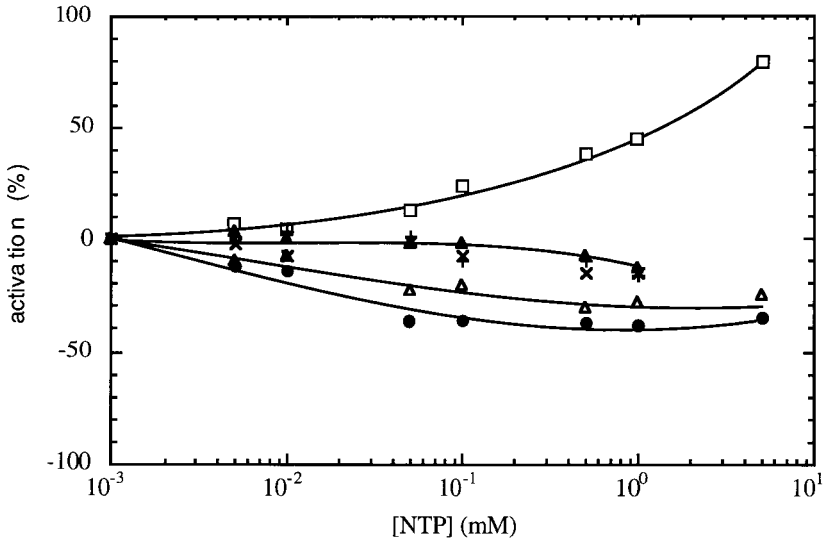

FIG. 3. Influence of nucleotide triphosphates on the activity of PyrBI and PyrB ATCases from *P. abyssi* produced in *E. coli*. ATCase activity in dialyzed cell extracts of *P. abyssi pyrBI* and *pyrB* clones expressed in *E. coli* JM103*pyrB*$^-$ was measured as described in Materials and Methods, in the presence of 3 mM aspartate. PyrBI ATCase (100 μg of protein): □, ATP; △, CTP; ●, UTP. PyrB ATCase (91 μg of protein): ▲, ATP; ×, CTP; +, UTP.

pKSAT3 clone, thereby eliminating the entire *pyrI* gene (Fig. 1). The protein encoded by the resulting *pyrB* subclone retained the ATCase activity. The potential involvement of the polypeptide encoded by *pyrI* in the allosteric regulation of this archaeal enzyme was investigated by comparing the influence of ATP, CTP, and UTP on the ATCase activity of dialyzed cell extracts of the *pyrBI* and *pyrB* clones (Fig. 3). The PyrBI ATCase of *P. abyssi* cloned in *E. coli* presented a pattern of allosteric response similar to that of the native enzyme from *P. abyssi* at 37°C (59): both CTP and UTP had an inhibitory effect, whereas ATP stimulated the activity. In contrast, the *P. abyssi* ATCase encoded by the *pyrB* subclone was insensitive to any of these three nucleotide triphosphates up to a concentration of 1 mM. Thus, the regulation by the nucleotide effectors requires the polypeptide encoded by the *pyrI* gene, which therefore is a regulatory chain. This was the first instance of an ATCase regulatory chain being characterized outside the *Enterobacteriaceae*. (Another archaeal PyrBI ATCase has since been discovered in the thermophile *Sulfolobus solfataricus* [accession no. X 99872] [12a].) However, the regulatory effects of the nucleotides are diminished when the archaeal enzyme is produced in *E. coli*. The maximal inhibition by CTP or UTP is 50% instead of 60% in the natural host (59), and the activation by ATP is 80% instead of 350% at a concentration of 5 mM (Fig. 3).

The cooperativity between catalytic sites for the utilization of aspartate is also reduced when *P. abyssi* ATCase is produced in *E. coli* (Hill number = 1.6 instead of 2.2 [59]). In the absence of regulatory chains, the *P. abyssi* ATCase did not exhibit cooperativity for binding of aspartate, indicating that, like in *E. coli* ATCase, this property requires the association of the catalytic and regulatory subunits.

Sequence comparison and analysis. (i) Nucleotide sequences. Comparison with 25 homologous genes shows that the *P. abyssi pyrB* and *pyrI* genes present the highest homology (59.4 and 58.7%, respectively) with the presumed homologous genes from the archaeon *Methanococcus jannaschii* (6). With eubacterial and eukaryal ATCases, the highest identities for *pyrB* are obtained with the corresponding enterobacterial gene from *Proteus vulgaris* (54.7%) (11), *E. coli* (54.2%) (11), *Serratia marcescens* (53.0%) (11), *Salmonella typhimurium* (52.5%) (11), and *Erwinia herbicola* (52.7%) (11), followed very closely by a large series of ATCase genes from eukaryotes comprising yeasts (*S. cerevisiae*, *S. pombe*) (41, 47), plants (*Arabidopsis thaliana*, *L. esculentum*, *Pisum sativum* sp.) (48, 54, 79), invertebrates (*Dictyostelium discoideum*, *Caenorhabditis elegans*) (18, 81), and vertebrates (*Squalus acanthias*, *Mesocricetus auratus*, *C. longicaudatus*) (27, 42, 68). The lowest identity of this archaeal *pyrB* gene is observed with the homologous gene from *Drosophila melanogaster* (38.2%) (19).

Alignment of the *pyrI* genes, necessarily restricted to the enterobacterial and *M. jannaschii* genes, provides, in the first case, identities slightly lower than those obtained for the alignment of *pyrB* genes (49.2 to 51.1%), while in the latter case these identity values are very close.

(ii) Amino acid sequences. Pairwise alignment of the deduced amino acid sequences of the *P. abyssi* ATCase polypeptide chains showed that the catalytic chain of the *P. abyssi* ATCase presents the highest identity and similarity, respectively, with the putative ATCase catalytic polypeptide from *M. jannaschii* (57.9 and 75.8%) and then with those from *P. vulgaris* (55.4 and 71.6%), *S. typhimurium* (51.5 and 71.1%), *E. coli* (53.5 and 71.3%), *S. marcescens* (51.8 and 70.9%), and *E. herbicola* (50.5 and 68.1%). High homology scores (greater than 50% identity) are also obtained with the eukaryotic ATCase catalytic chains from *L. esculentum* and *P. sativum pyrB*1. The lowest percent identity and similarity is obtained with *D. melanogaster* ATCase (29.4 and 53.1%, respectively). For the regulatory chain, comparison of the *P. abyssi* sequence with those of the corresponding enterobacterial chains shows lower identities (41.3 to 44.3%) and similarities (65.3 to 67.1%) than between the catalytic chains from the same organisms. In contrast, a very high identity and similarity were obtained with the protein encoded by the *pyrI* gene of *M. jannaschii* (56.2 and 76.0%).

A multiple alignment of the *P. abyssi* amino acid sequences of the catalytic and regulatory chains with the homologous chains of the enterobacterial ATCases (*E. coli*, *S. marcescens*, *S. typhimurium*, *P. vulgaris*, and *E. herbicola*) is shown in Fig. 4. Catalytic-chain comparison (Fig. 4a) reveals that 41.6% of the residues fully conserved in *Enterobacteriaceae* are also present

(a)

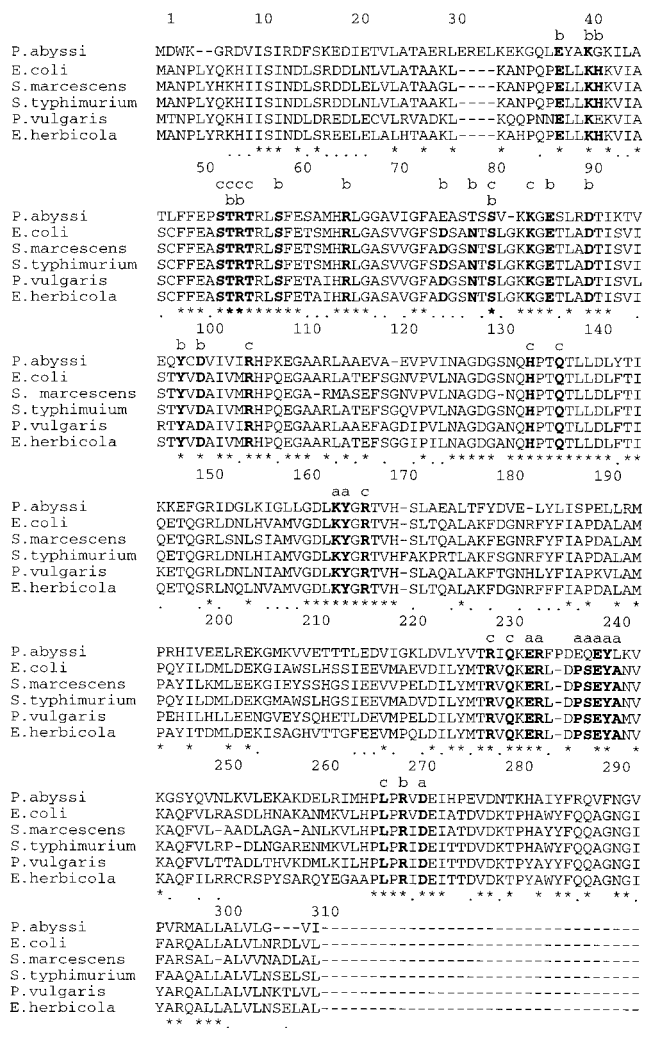

(b)

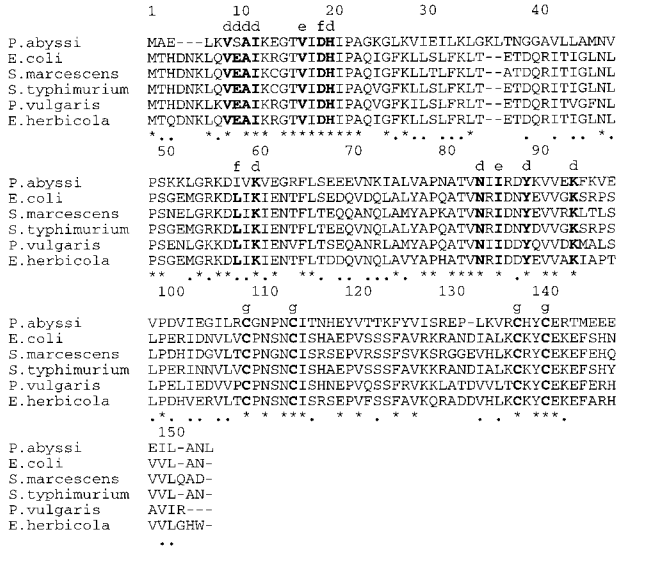

FIG. 4. Multiple alignment of the amino acid sequences of *P. abyssi* and enterobacterial ATCases. (a) Catalytic chains. Conservation of the residues which, in *E. coli* ATCase, form the catalytic site (top line, c), the c1-c4 interface in T state (top line, a), or the c1-c2 interface in T and R state (top line, b) is indicated. (b) Regulatory chains. Conservation of the residues which in *E. coli* ATCase are common to ATP and CTP binding (top line, d), specifically involved in the ATP binding (top line e), specifically involved in the CTP binding (top line, f), or implicated in the coordination of the Zn atom (top line, g) is indicated. *, identical residues; ·, conservative substitutions.

in *P. abyssi*, while 36.3% are changed. Overall, these catalytic chains show 65.2% similarity. Analysis of the regulatory chain reveals 35.5% identity and 61.8% similarity with the homologous enterobacterial polypeptides (Fig. 4b). A total of 40% of the residues conserved in enterobacterial ATCase regulatory chains are replaced in *P. abyssi*. These values indicate a stronger conservation of the primary structure of the catalytic chain than of the regulatory chain.

(iii) Catalytic site. The most striking observation which emerges from the comparison of the ATCase catalytic chains of ATCases from 25 species is the complete conservation of the specific residues which were shown in *E. coli* to constitute the catalytic site (23, 44). This conservation extends to *P. abyssi* ATCase (Fig. 4a).

(iv) Regulatory site. In *E. coli* ATCase, the allosteric effectors ATP, CTP, and UTP bind competitively to the same regulatory sites (28, 29). *P. abyssi* ATCase is regulated by the same nucleotides, although it is not known whether they bind to the same sites (59). Figure 4b shows that most of the residues forming the nucleotide binding site in *E. coli* ATCase (70) are conserved in the *P. abyssi* regulatory chain. Val 9, Glu 10, Ala 11, Ile 12, His 19, Lys 60, Asn 84, Tyr 89, and Lys 94, common to the binding site of the three nucleotides in *E. coli*, are all conserved in *P. abyssi*, except for Glu 10, which is replaced by a lysine residue. (All residue numbers refer to the amino acid sequence of the *E. coli* ATCase.) CTP binding involves in addition Val 17 and Ile 86, which are also both conserved in *P. abyssi*. ATP binding implicates specifically two residues, Asp 19, which is conserved, and Leu 58, which is replaced by isoleucine in *P. abyssi*. Thus, these results suggest that in *P. abyssi* ATCase the three nucleotides bind to the same regulatory sites and that this binding involves basically the same residues as in the *E. coli* regulatory chain.

(v) Metal-binding cysteine residues. In enterobacterial ATCases, four cysteine residues are clustered in the C-terminal region of the regulatory chain. They bind a Zn atom whose presence is required for the association of the catalytic and regulatory subunits (24). These cysteines are present at the same positions in the *P. abyssi* regulatory chain (Fig. 4b), suggesting that this archaeal ATCase is also a metalloprotein.

Amino acid composition and thermostability. Previous work showed that ATCase from *P. abyssi* is highly thermostable compared to the homologous *E. coli* enzyme (59). Structural studies of enzymes from thermophilic and hyperthermophilic microorganisms led to the proposal of several types of modification possibly responsible for the increased thermostability of proteins. These include additional ionic bonds; increased packing of hydrophobic cores resulting from the presence of bulkier hydrophobic residues; a decreased number of thermolabile residues such as tryptophan, glutamine, asparagine, and cysteine; and an increased number of proline residues (43). Alpha-helices can be stabilized by the presence of charged residues in N-caps (50, 51, 60). Several primary structure features of both catalytic and regulatory chains of the *P. abyssi* ATCase (Table 1) might contribute to its thermal stability.

(i) Catalytic chain. The archaeal catalytic chain presents a significantly increased number of charged residues in comparison with the *E. coli* homologous chain (21 arginines, 24 lysines, and 31 glutamates instead of 15, 15, and 14, respectively). Examination of the hydrophobic residues shows that there are more valines (28 versus 22) and fewer alanines (20 versus 34) in the *P. abyssi* polypeptide than in the corresponding *E. coli* chain, indicating a difference in the hydrophobicity of this chain. The occurrences of thermolabile residues asparagine, glutamine, and tryptophan are considerably lower than in *E. coli* ATCase (5 versus 15, 8 versus 14, and 1 versus 2, respectively).

(ii) Regulatory chain. Comparison of the *P. abyssi* and *E. coli* regulatory chains revealed a divergence similar to that observed for the catalytic chains. The numbers of glutamate and lysine charged residues are increased in the hyperthermophilic polypeptide (17 versus 10 and 16 versus 11, respectively), although the number of aspartate residues decreases by more than 50% (4 versus 9). Different numbers of valine (18 versus 12), glycine (10 versus 6), and serine (4 versus 11) residues were also observed, as well as the remarkable absence of glutamine (0 versus 6). In both catalytic and regulatory chains of *P. abyssi* and *E. coli*, the number of cysteines is constant (1 versus 1 and 4 versus 4, respectively) and the number of prolines is virtually unchanged (11 versus 12 and 6 versus 7, respectively).

HCA. An increased packing of the hydrophobic cores was also proposed as one of the possible causes of increased protein thermostability (21, 43). The significant differences in the numbers and locations of the hydrophobic residues in the *P. abyssi* and *E. coli* proteins (Table 1 and Fig. 4) were analyzed by the HCA method (20, 38). The results are shown in Fig. 5.

(i) Catalytic chain. Analysis of the catalytic chain of *P. abyssi* revealed two hydrophobic clusters whose size and packing are increased with respect to *E. coli*. The first one comprises the region from positions 135 to 193 (substitutions Gln 149→Phe, Lys 178→Phe, Gly 180→Val, Arg 183→Leu, and Ala 192→Leu). The second region corresponds to the carboxyl end, starting at residue 285 (substitutions Ala 289→Val, Gly 290→Phe, Ala 295→Val, and Gln 297→Met). In addition, because of the absence in *P. abyssi* of residues 306 to 308 of the *E. coli* protein, the terminal valine and isoleucine residues become part of this hydrophobic cluster. In these two regions, changes in the nature of the hydrophobic residues are also observed. It is important that although these two regions are far apart in the primary structure of the catalytic chain, they are close to each other in the tridimensional structure and they both contribute to the formation of the catalytic site (33).

(ii) Regulatory chain. In the regulatory chains, three regions showed changes in hydrophobicity: the vicinity of the regulatory site (insertion of Leu 35 and Lys 36 and Arg 41→Leu), the loop which links the allosteric and the zinc domains (Arg 85→Ile, Ser 95→Phe, and Pro 97→Val), and the stretch of residues between the two groups of cysteines coordinating the metal atom (Pro 120→Tyr, Ala 126→Tyr, and Arg 128→Ile). The pattern of hydrophobicity of the region from positions 51 to 79 (S3′ and H2′ in *E. coli*, where H refers to the alpha-helix and S refers to the β-strand) is conserved in spite of numerous substitutions.

Secondary structure prediction. The PHDsec program (61–63) provided a good prediction for the known secondary structure of the *E. coli* ATCase catalytic chain (PyrB) and was therefore used to predict the secondary structure of the catalytic chain of *P. abyssi*. These secondary structures are compared in Fig. 6. They present very similar alpha-helix and β-strand organizations. However, a few differences are observed, such as a 4-amino-acid insertion in helix H1; the absence of strands S8, S10, and S11; and a rearrangement and shortening of the region H11-H12. A Pro→Glu substitution at the amino terminus of H9 might contribute to an increase in the thermal stability of *P. abyssi* ATCase through an N-cap interaction (50, 51).

TABLE 1. Amino acid compositions of *P. abyssi* and *E. coli* ATCases

Residue	No. of amino acids[a]							
	Catalytic chain			Regulatory chain			Total	
	P. abyssi		*E. coli*	*P. abyssi*		*E. coli*	*P. abyssi*	*E. coli*
Ala	20	−	34	9		10	29	44
Arg	21	+	15	7		8	28	23
Asp	17		21	4	−	9	21	30
Asn	5	−	15	9		11	14	26
Cys	1		1	4		4	5	5
Glu	31	+	14	17	+	10	48	24
Gln	8	−	14	0	−	6	8	20
Gly	20	+	15	10	+	6	30	21
His	8		11	3		4	11	15
Ile	20		15	14		12	34	27
Leu	36		38	14		15	50	53
Lys	24	+	15	16	+	11	40	26
Met	6		9	3		2	9	11
Phe	10		12	3		5	13	17
Pro	11		12	6		7	17	19
Ser	13	−	20	4	−	11	17	31
Thr	18		18	7		7	25	25
Trp	1	−	2	0		0	1	2
Tyr	10		8	4		3	14	11
Val	28	+	22	18	+	12	46	34

[a] Arrows indicate the most significant changes in amino acid composition. + and −, more or less abundant, respectively, in the *P. abyssi* polypeptide than in the *E. coli* polypeptide.

Because of the looser structural organization of the *E. coli* ATCase regulatory chain, the program gave a poor prediction of its secondary structure. Consequently, it was not used for the analysis of the *P. abyssi* PyrI chain.

Modeling of the tridimensional structure of the catalytic chain. The high degree of homology of the primary and secondary structures of the *P. abyssi* ATCase with that of the *E. coli* enzyme allowed modeling of the tridimensional structure of the archaeal enzyme on the basis of the known crystallographic structure of the *E. coli* protein.

Figure 7 (top) shows the superposition of the structure obtained for the *P. abyssi* catalytic chain and the crystallographic structure of the *E. coli* protein. These two structures are closely related. In particular, the carbamylphosphate binding domain (left) and the aspartate binding domain (right) are present and similarly folded in the two proteins. However, several significant differences are observed. The three major changes concern the region of helix H1, the 80 loop in the carbamylphosphate binding domain, and the 240 loop in the aspartate binding domain. The first one is related to the 4-residue inser-

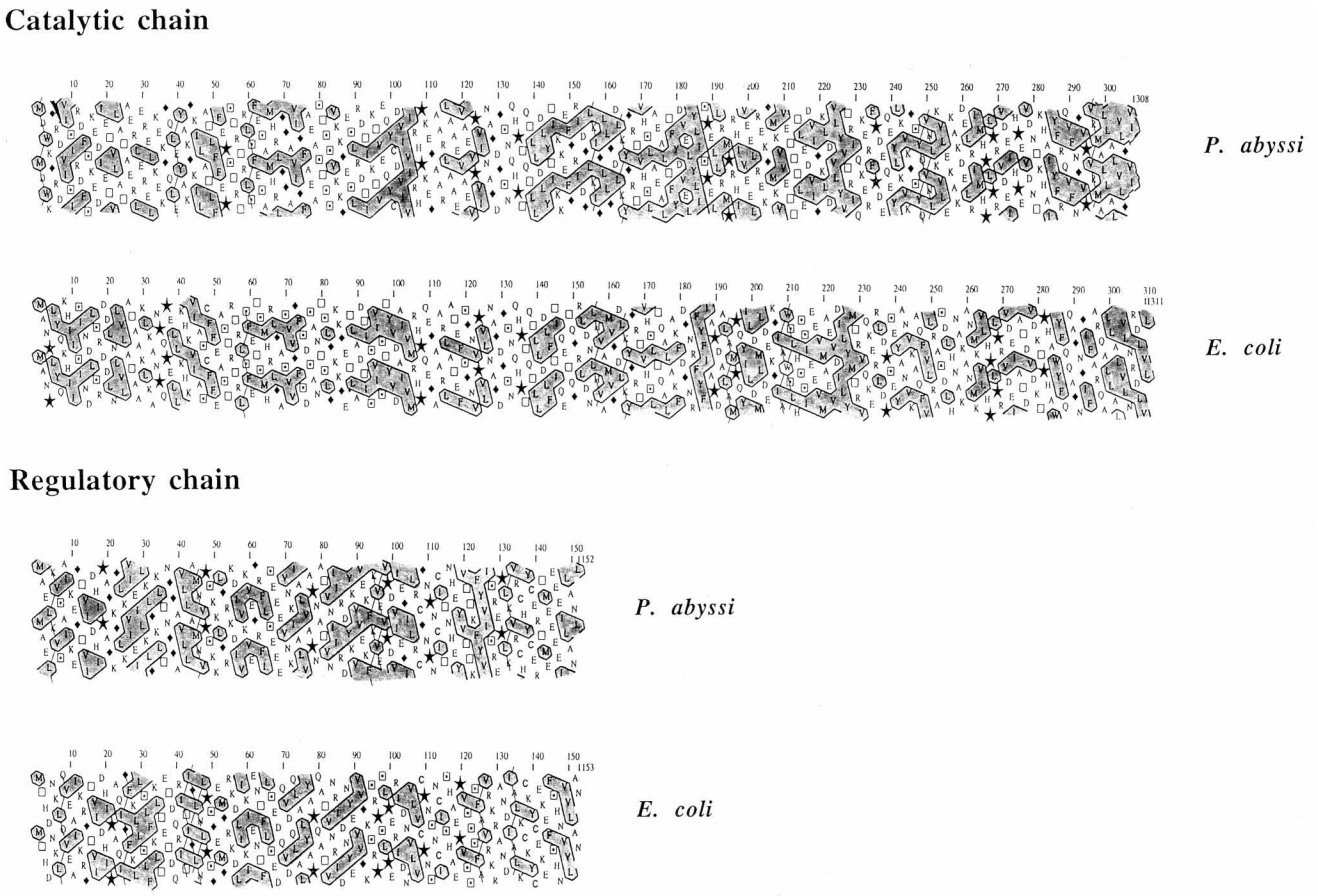

FIG. 5. Comparison of the HCA plots of the catalytic and regulatory chains of *P. abyssi* and *E. coli* ATCases. The sequences are written on a classical alpha-helix (3.6 amino acids per turn) smoothed on a cylinder. To make the three-dimensional representation easier to handle, the cylinder is cut parallel to its axis and then spread out. Since some adjacent amino acids are now separated by the unfolding of the cylinder, their representation is duplicated to restore the full connectivity of each amino acid. Clusters of adjacent hydrophobic residues are then contoured and shaded: ★, proline; ◆, glycine; ⊡, serine; □, threonine.

tion present in the *P. abyssi* enzyme (Fig. 4a), which appears to alter the organization of H1. The other important differences are the rotations of the 80 and 240 loops. As a consequence of these reorientations, the charged residues Lys 80, Lys 227, and Arg 229 (residue numbers in the *P. abyssi* enzyme) are exposed to the solvent.

Figure 7 (bottom) shows the localization of all the additional charged residues which are present only in the *P. abyssi* catalytic chain, relative to the *E. coli* protein. Strikingly, all these residues are located at the surface of the protein and point to the exterior of the catalytic chain. Therefore, they are potentially involved in the reinforcement of the interactions between chains and/or subunits in the quaternary structure of the *P. abyssi* ATCase.

In the case of the regulatory chain, the Swiss-Model program could not provide a valid modeling, again because of important differences in the secondary and tertiary structures of this type of chain in the *P. abyssi* and *E. coli* enzymes.

Conservation of the pairs of residues involved in inter- and intrachain interactions. The high degree of conservation of the primary and secondary structures between *P. abyssi* and *E. coli* ATCases and the modeling of the catalytic chain suggest that these two enzymes have comparable tridimensional structures. Therefore, the conservation in the *P. abyssi* enzyme of the pairs of residues whose side chains are involved in interactions between chains or between domains of these chains in *E. coli* ATCase (32, 40) was investigated. The results obtained are shown in Table 2. Interestingly, 9 of 11 of the amino acid pairs involved in the interactions between the catalytic chains within a trimeric catalytic subunit in *E. coli* (c1-c2 interface) (70) are conserved in *P. abyssi*. All seven pairs of residues of the *E. coli* ATCase involved in the contact between catalytic chains belonging to different catalytic trimers in the T state (c1-c4 interface) (70) are also present in *P. abyssi*, while the two pairs of residues of this interface present in the R state are changed (Table 2). The residues involved in these two types of interface are also shown in Fig. 4a. These conservations suggest similar arrangements of the catalytic chains and subunits in the two enzymes.

In contrast, there is virtually no conservation of the interactions between regulatory chains within the regulatory dimer (r1-r6 interface), in spite of 43.6% identity between the amino acid sequences of the regulatory chains of *P. abyssi* and *E. coli*, suggesting again a significant difference in the three-dimensional structures of the regulatory chains of these two organisms.

In *E. coli* ATCase, the interactions between the catalytic and regulatory subunits involve two types of interfaces. The r1-c1 interface links a regulatory chain to a catalytic chain of the catalytic trimer which belongs to the same half of the ATCase molecule. Of 11 pairs of amino acids involved in this interface, 9 are conserved in *P. abyssi* PyrB and PyrI chains. The second

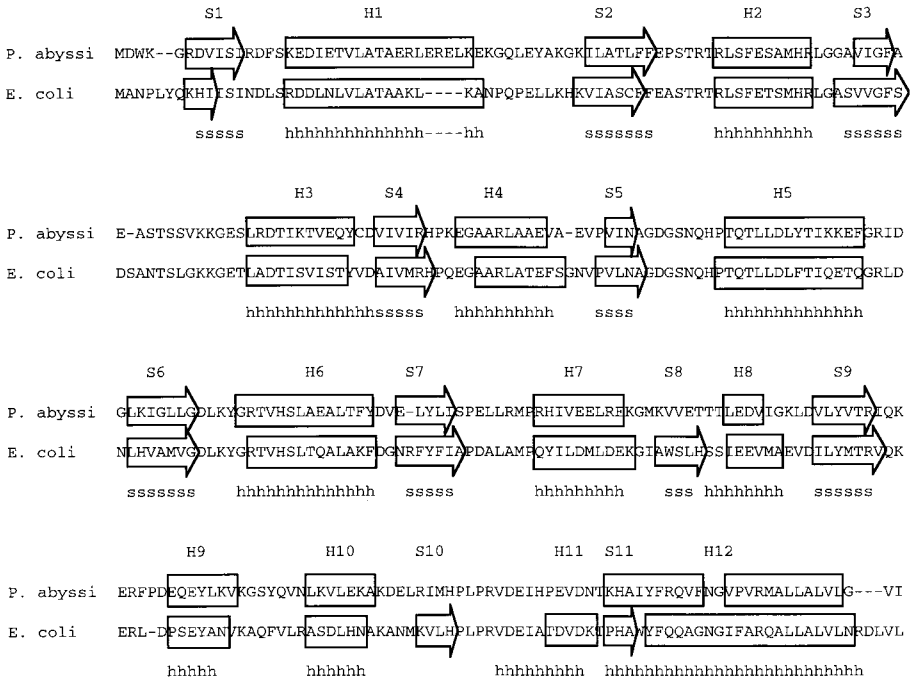

FIG. 6. Comparison of the predicted secondary structure of the ATCase catalytic chain from *P. abyssi* with the secondary structure of the *E. coli* protein, known from crystallography. Alpha-helices (boxes) and β-strands (arrows) are indicated. The secondary structure of the *E. coli* chain predicted with the same program is shown underneath. h, alpha-helix; s, β-strand.

type of interface, r1-c4, links a regulatory chain to a catalytic chain of the catalytic trimer which belongs to the other half of the *E. coli* ATCase molecule. Interestingly, in the *P. abyssi* enzyme, the amino acid pairs corresponding to this interface are much less conserved.

Good conservation of the pairs of amino acids forming the carbamylphosphate-aspartate interface of the *E. coli* catalytic chain is observed (8 of 11) (Table 2). Again, a lower degree of conservation is observed in the regulatory chain of *P. abyssi* ATCase: of 12 pairs of residues involved in the allosteric domain-Zn domain interface in the *E. coli* enzyme, only 4 are conserved.

Thermostability and barostability of *P. abyssi* ATCase and its catalytic subunits produced in *E. coli*. *P. abyssi* ATCase is highly thermostable. Indeed, preincubation at 90°C of dialyzed cell extracts of *P. abyssi* for at least 6 h does not provoke any inactivation (59). This thermostability was also investigated in dialyzed cell extracts of the recombinant *E. coli* mutant JM103*pyrB*$^-$ containing the *P. abyssi pyrBI* or *pyrB* clones. These extracts were incubated at 90°C for 20 min, and the residual ATCase activity was measured at 37°C. The results are shown in Fig. 8. The ATCase from *P. abyssi* cloned in *E. coli* retained activity, but its stability was lower than that in extracts of its native host. A 20-min incubation at 90°C partially inactivated this enzyme to 40% of its initial activity, and then the activity reached a plateau, remaining constant for at least 6 h (data not shown). Under the same conditions, the catalytic subunits from the *P. abyssi pyrB* clone preserved 60% of their activity. This thermostability is still remarkable, since under the same conditions the mesophilic *E. coli* ATCase was completely inactivated after 2 min (Fig. 8).

P. abyssi is a deep-sea archaeon which thrives naturally under a hydrostatic pressure of 20 MPa, and it was shown previously that the ATCase from this organism is resistant to hydrostatic pressure up to at least 200 MPa (59). Under the same conditions, the *E. coli* enzyme is inactivated very rapidly (unpublished data). The stability to hydrostatic pressure of the ATCase and catalytic subunits from *P. abyssi* cloned in *E. coli* was determined by incubation of dialyzed cell extracts for 10 min at increasing pressures followed by measurement of the ATCase activity at atmospheric pressure. As shown in Fig. 9a, pressure partially inactivated both these enzymes down to a plateau corresponding to about 30% of their initial activity. Under similar conditions, the *E. coli* ATCase was completely inactivated (26a). Thus, the enzyme cloned in *E. coli* exhibits a lower barostability than the native *P. abyssi* ATCase. Interestingly, when the extract containing *P. abyssi* ATCase previously incubated under pressures up to 300 MPa was further incubated at 90°C under atmospheric pressure, recovery of the initial activity was observed (Fig. 9b). This activation did not occur in the case of the *P. abyssi* clone coding only for the catalytic subunits. The significance of this phenomenon will be investigated further.

DISCUSSION

The ATCase genes of the deep-sea hyperthermophilic archaeon *P. abyssi* were cloned, sequenced, and expressed in *E. coli*. This is the first characterization of an archaeal gene coding for this enzyme. Unexpectedly, in *P. abyssi*, ATCase is encoded by two genes, *pyrB*, coding for the catalytic chain, and *pyrI*, coding for a regulatory chain. These two genes are adjacent and might constitute an operon. Until recently, regulatory chains had been found only for enterobacterial ATCases and, possibly, in the archaeon *M. jannaschii*. However, in the latter organism, the ATCase genes are located at different sites on the chromosome (6). Contrary to what is observed in enterobacterial *pyrBI* operons, *P. abyssi* does not possess an intercistronic region between *pyrB* and *pyrI*. This might be related to the existence of a translational coupling between *pyrB* and *pyrI*

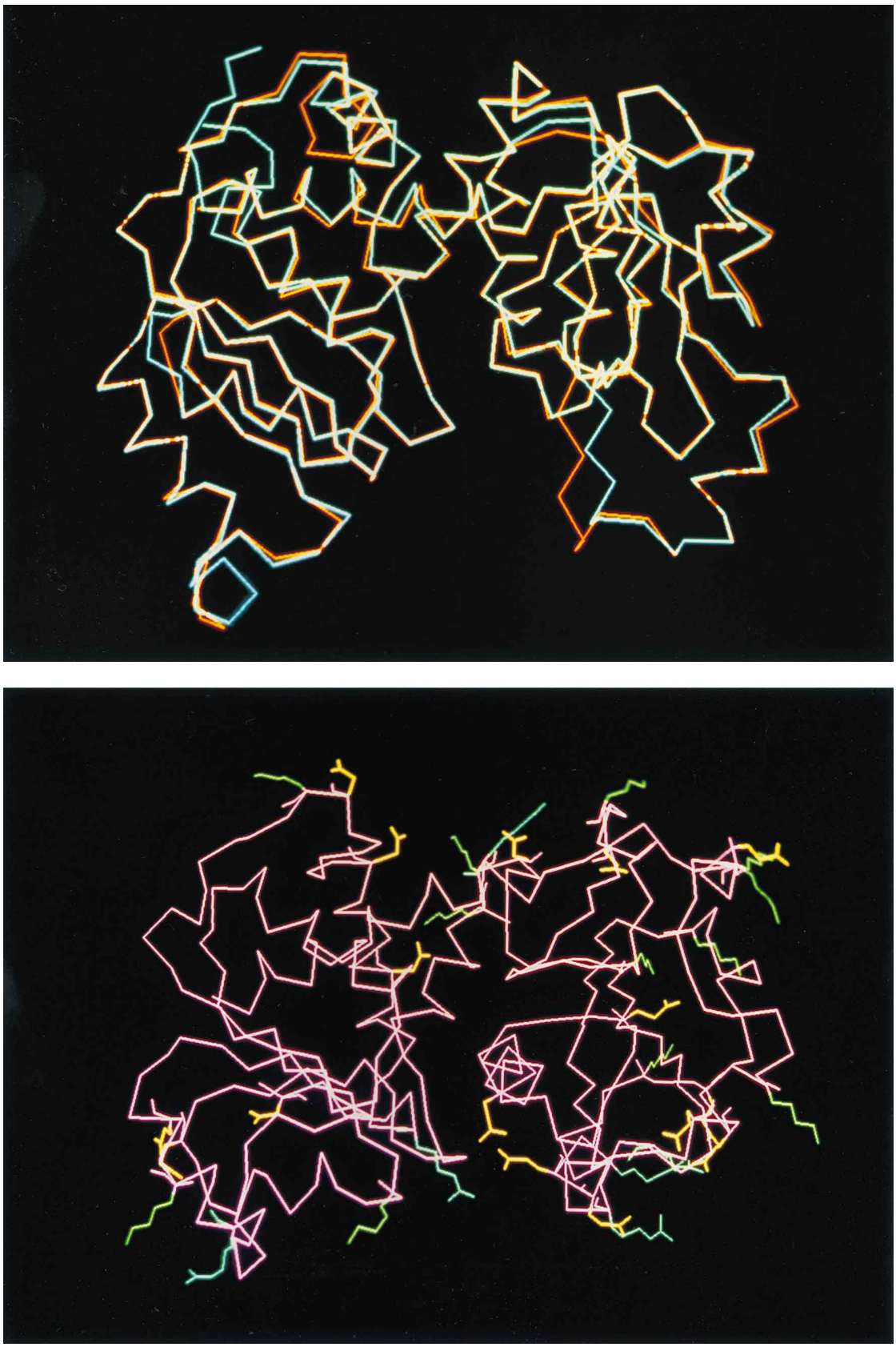

FIG. 7. Three-dimensional modeling of the *P. abyssi* ATCase catalytic chain. (Top) Superposition of the backbone of the predicted *P. abyssi* catalytic chain structure (orange) with that of the *E. coli* protein (blue) obtained from crystallographic data. The left region corresponds to the carbamylphosphate binding domain with the 80 loop at the bottom, and the right region corresponds to the aspartate binding domain containing the 240 loop at the bottom. These two loops are oriented differently in the *P. abyssi* and the *E. coli* ATCases. Cream color indicates perfect superposition. (Bottom) Additional charged residues in the *P. abyssi* ATCase catalytic chain relative to the *E. coli* polypeptide. Green, lysine and arginine residues; yellow, aspartate and glutamate residues. The modeling of the *P. abyssi* catalytic chain begins at residue 6.

TABLE 2. Conservation in *P. abyssi* ATCase of pairs of interacting residues at the inter- and intrachain interfaces in the *E. coli* enzyme[a]

Interface	Conformational state	Interface	Conformational state	Interface	Conformational state
c1-c2		c1-c4		r1-r6	
D90-R269	TR	D271-Y240*	T	R55-D39(G)	TR
D90-R65	T	E239-Y165	T	Q24(G)-D39(G)	T
E86-R54	TR	E239-K164	T	Q24(G)-T38(N)	T
D100-R65	TR	R234-R234	T	N47-Q40(G)	T
Y98-S58	T	E233-R234	T	N47-T38(N)	TR
Y98-R65	R	K164-E239	T	N47-D39(G)	R
S80-T53	T	Y165-E239	T	L46(M)-I42(V)	TR
H41(G)-E37	TR	A241(L)-S238(Q)	R	I42(V)-L46(M)	TR
K40-E37	T	*P237(E)-Y240	R	T38(N)-N47	T
N78(T)-D75(E)	R			T38(N)-Q24(G)	R
G85-V270	T			D39(G)-N47	TR
				D39(G)-R55	TR
				Q8(K)-E10(S)	R
				V9-E10(S)	R
				I44(L)-I44(L)	R
r1-c1		r1-c4			
K139(H)-E117	TR	K143(R)-D236	T		
E142-N13	T	K143(R)-S238(Q)	T		
E142-S11	TR	N111-S238(Q)	T		
E142-N132	TR	E144(T)-N242(K)	T		
E142-R113	R	S146(E)-N242(K)	T		
K143(R)-S131	T	N148(E)-K244	T		
N111-E109	TR				
N113-E109	TR				
N113-Q108(K)	TR				
Y140-E117	R				
C141-N132	R				
CP-aspartate[b]		Allosteric domain-Zn domain			
K31-Q147(K)	T	Q73(K)-R102(V)	T		
R17-D153	TR	Q73(K)-I103	T		
R17(K)-D180	TR	Q73(K)-D104(E)	T		
Q137-D141	T	Y77(V)-V106(I)	T		
N13(R)-Q174(E)	TR	L76-L151	TR		
H134-S171	R	Y77(V)-L151	TR		
Q133-Q174(E)	R	K28-L151	T		
Q133-S171	R	P100-V127	R		
E50-R167	R	P100-K129(S)	R		
E50-R234	R	L99(V)-K129(S)	R		
I12-S171	R	K28-N153	R		

[a] *, residues belonging to the same chain (c1 or c4). Letters in parentheses indicate residues in *P. abyssi* ATCase which are substituted with respect to the *E. coli* enzyme.
[b] CP, carbamylphosphate.

in *P. abyssi*. Recent data show that another archaeal ATCase from the extreme thermophile *S. solfataricus* is also coded for by a *pyrB* gene and a *pyrI* gene (accession no. X 99872 [12a]).

The ATCase amino acid sequence shows a remarkably high degree of identity and similarity with the homologous enzymes from bacteria to mammals (47 to 58% identity; 65 to 76% similarity). The highest homology is found with *M. jannaschii* (particularly between the regulatory chains) and then with the *Enterobacteriaceae*, suggesting that these archaea and the *Enterobacteriaceae* are evolutionarily close. The regulatory chain shows more-extensive divergence with respect to that of *E. coli* and other *Enterobacteriaceae* than the catalytic chain. Unexpectedly, the *P. abyssi* sequence shows low homology with those of the thermophilic and hyperthermophilic eubacterial ATCases from *T. aquaticus* and *Thermotoga maritima* (73, 74).

In the regulatory chain of *P. abyssi*, the four cysteine residues, which in *E. coli* are involved in the binding of a zinc atom, are conserved. This feature suggests that *P. abyssi* ATCase is also a metalloprotein. However, considering the very peculiar composition of the hydrothermal vent fluid, the coordinated metal might not be zinc in this case.

P. abyssi ATCase is very thermostable (59). In comparison with the *E. coli* enzyme, it shows several structural features potentially related to its thermostability.

(i) It contains 34 additional charged residues, which might form an increased number of ionic bonds. The modeling showed that in the catalytic chain, all these additional charged residues are located at the surface of the protein and point to its exterior, which makes it very likely that they are involved in the interactions between chains and/or subunits.

(ii) It also contains 13 additional hydrophobic residues, and some others are replaced by bulkier residues. The HCA shows that these modifications increase the size and probably the packing of the hydrophobic clusters.

(iii) It presents a decreased number of thermolabile residues, Asn, Gln, and Trp (25 fewer).

The above observations suggest that the increased size and packing of the hydrophobic clusters would stabilize the cata-

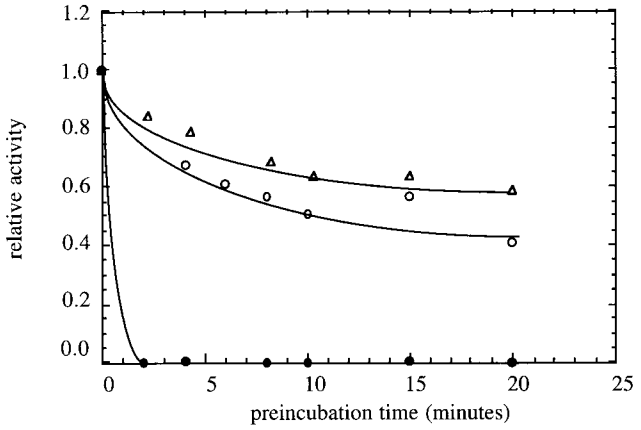

FIG. 8. Influence of temperature on the stability of the *P. abyssi* PyrBI and PyrB ATCases produced in *E. coli*. The different dialyzed cell extracts were incubated at 90°C for up to 20 min. Samples were taken, and their ATCase activity was measured at 37°C. △, *P. abyssi* PyrB (33 μg at 16.7 mg/ml); ○, *P. abyssi* PyrBI (39 μg at 19.5 mg/ml); ●, *E. coli* PyrBI (0.2 μg at 0.1 mg/ml).

lytic monomer, while the numerous additional charged residues would instead be involved in the stabilization of the quaternary structure of the archaeal enzyme.

When the *P. abyssi* ATCase operon was expressed in *E. coli*, the enzyme appeared to be significantly less thermostable and barostable than in its natural host. Furthermore, a reduction of cooperativity and allosteric effects was observed. Since such alterations were also observed during the different steps of purification of the native enzyme, these results suggest that in *P. abyssi* the ATCase might be stabilized in part by association with another cellular component. It was shown that in *P. abyssi* cell extracts the heat-labile metabolite carbamylphosphate is channelled from the catalytic sites of CPSase to those of ATCase, where it is used as a substrate (58). A similar observation was made for *Pyrococcus furiosus* (37). Therefore, the high degree of stability of *P. abyssi* ATCase in cell extracts of the same species might result in part from its transient association with CPSase and/or other enzymes of the pyrimidine pathway. Nevertheless, a modified folding of the protein when translated in the *E. coli* host is not excluded.

There is no information so far about the structural modifications which are able to increase the barostability of proteins, and it is not possible yet to speculate on the structural features which in the *P. abyssi* ATCase might be involved in this stabilization. In this regard, it will be interesting to compare the *P. abyssi* ATCase to that of *P. furiosus*, which lives at atmospheric pressure.

The prediction of the secondary structure of the *P. abyssi* catalytic chain showed a high level of similarity with that of the *E. coli* protein, with some differences located in the aspartate binding domain. All the alpha-helices are present, an observation which is corroborated by the predicted tridimensional structure.

In *E. coli*, the catalytic sites are located at the interfaces between two catalytic chains belonging to the same catalytic trimer (c1-c2 interfaces). In each catalytic site, residues Ser 80 and Lys 84 are contributed by one chain and the other residues are contributed by the adjacent chain (36). Since all these residues are conserved in the *P. abyssi* ATCase, its catalytic site should also be at the interface between two catalytic chains. In addition, the pairs of residues which are involved in the interactions at the c1-c2 interface in *E. coli* are almost entirely conserved. Taken together, these observations indicate that in *P. abyssi*, the catalytic chains should be associated also into catalytically active trimers. The modeled three-dimensional structure of the catalytic chain of *P. abyssi* can be superimposed on the known crystallographic structure of the catalytic chain of *E. coli* ATCase (Fig. 8), although there are significant differences in the 80 and 240 loops and in helix H1.

The amino acid pairs involved in the r1-c1 type of interface which in the *E. coli* ATCase contribute to the association of catalytic and regulatory subunits are almost entirely conserved in the *P. abyssi* enzyme (9 of 11), suggesting that this interface contributes to the establishment of the quaternary structure of this archaebacterial ATCase. Taken together, the similarities of the secondary and tridimensional structures and the conservation of the amino acid pairs involved in chain and subunit interactions strongly suggest that the two enzymes have a similar quaternary structure.

In *E. coli* ATCase, the transition from a T state to an R state with different affinities for aspartate is the basis for the cooperativity between catalytic sites for aspartate binding. The c1-c4 interface is severely disrupted during the T-to-R transition, and in R-state *E. coli* ATCase, the only remaining c1-c4 interactions involve four residues of the 240 loop of the catalytic chains (33). These pairs of residues are substituted in the

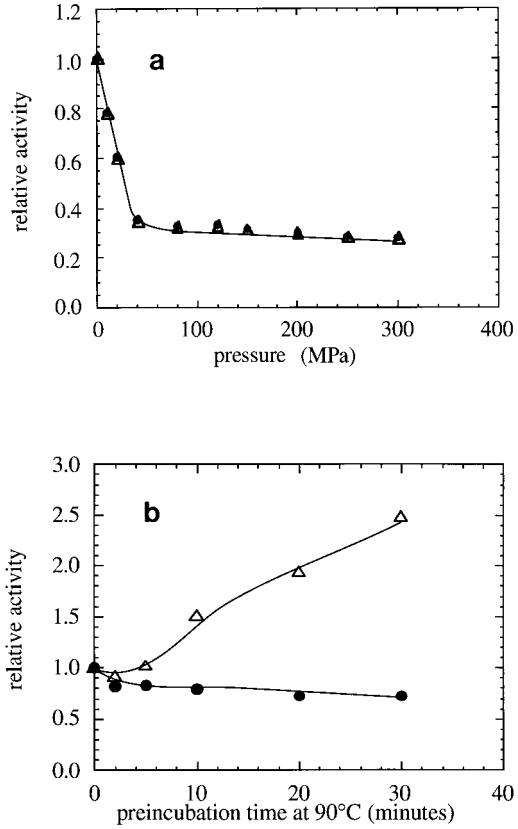

FIG. 9. Influence of pressure on the stability of the *P. abyssi* PyrBI and PyrB ATCases produced in *E. coli*. (a) Each dialyzed cell extract (33 mg at 1.9 mg/ml for PyrBI and 35 mg at 2.1 mg/ml for PyrB) was incubated under increasing hydrostatic pressures. Increases of pressure occurred every 10 min. Samples were taken (578 μg of PyrBI and 622 μg of PyrB) at the end of each step, and their ATCase activity was immediately measured at atmospheric pressure and 37°C (Materials and Methods). (b) Extracts incubated as described above up to 300 MPa (57 μg of PyrBI and 63 μg of PyrB) were further incubated at 90°C for up to 30 min. Samples were taken, and their ATCase activity was measured at 37°C under standard conditions. △, *P. abyssi* PyrBI; ●, *P. abyssi* PyrB.

archaeal enzyme. These differences, as well as the different orientations of the 240 and 80 loops in the *P. abyssi* ATCase (Fig. 7), might be related to the reduced cooperativity for aspartate binding exhibited by this enzyme. In addition, the different orientation of the 80 loop, whose residues interact with both substrates in the *E. coli* ATCase, might be related to the channeling of carbamylphosphate in the *P. abyssi* enzyme.

As far as the allosteric regulation is concerned, most of the amino acids which are involved in the binding of ATP, CTP, and UTP to the regulatory sites of *E. coli* ATCase (71) are conserved in the *P. abyssi* enzyme, which probably explains the sensitivity of this enzyme to the same effectors. However, the mechanisms of action seem different in the two enzymes.

(i) For *E. coli* and other enterobacterial ATCases, the mechanism of transmission of the regulatory signal of the activator ATP has been partially deciphered (9, 12, 72, 82, 83). It involves well-defined interactions at the interfaces between the two domains of the regulatory chain (allosteric and zinc domains), as well as between the regulatory and the catalytic subunits (r1-c4). Since the residues involved in these interactions are poorly conserved in the *P. abyssi* ATCase, the ATP regulation might act through a different mechanism.

(ii) It was shown that in *E. coli* ATCase the synergy of action of the feedback inhibitors CTP and UTP is based on positive and negative cooperativity between the two regulatory sites of the regulatory dimers. This involves transmission of conformational signals through the r1-r6 type of interface (13, 14). The lack of CTP-UTP synergy in *P. abyssi* ATCase might be related to the very poor conservation of the pairs of amino acids involved in this interface (Table 2).

The presence of a regulatory chain in the archaeal ATCase is remarkable, since so far it has been found only in the corresponding enterobacterial enzymes. In *E. coli* ATCase, the regulatory subunits are considerably less thermostable than the catalytic subunits (34). Consequently, adaptation of ATCase containing regulatory chains to high temperatures should have required more-substantial modifications of the regulatory chains than of the catalytic chains. This interpretation is supported by the higher degree of divergence between the *P. abyssi* and enterobacterial ATCase regulatory chains than between the catalytic chains and by the very high degree of identity and similarity between the ATCase regulatory chains of the hyperthermophilic archaea *P. abyssi* and *M. jannaschii*. This stabilization of the regulatory chains might not have been compatible with the maintenance of the mechanisms of action of the allosteric effectors which operate in *Enterobacteriaceae*, and the adaptation of the ATCase feedback regulation to high temperatures might have led to the emergence of new mechanisms of action of the allosteric effectors in the *P. abyssi* enzyme.

ACKNOWLEDGMENTS

We are indebted to Bart Scherens (CERIA) and Martine Roovers and Marc Van de Casteele (Microbiology, VUB, VIB) for helpful discussions and assistance with some of the protocols and to Jacques Chomilier, Luc Canard, and Jean-Paul Mornon for their help in performing the HCA.

This work was supported by a contract between the Flemish Interuniversity Institute for Biotechnology (VIB) and the Laboratory for Genetics and Microbiology (Erfelijkheidsleer en Microbiologie) of the VUB, by CNRS, and by grants G.0040.96 from the Belgian (Flanders) Nationaal Fonds voor Wetenschappelijk Onderzoek and 1-96-3-21-145-0 from the Onderzoeksraad (OZR) of the VUB. C. Purcarea was supported by a grant from the OZR of the VUB to R.C. and by short-term fellowships from the Federation of European Biochemical Societies (FEBS) and from the International Human Frontier Science Program (HFSP) (SF-339/94).

REFERENCES

1. **Ahonkhai, I., M. Kamekura, and D. J. Kushner.** 1989. Effects of salts on the aspartate transcarbamylase of a halophilic eubacterium, *Vibrio costicola*. Biochem. Cell. Biol. **67:**666–669.
2. **Allen, C. M. J., and M. E. Jones.** 1964. Decomposition of carbamylphosphate in aqueous solutions. Biochemistry **3:**1238–1247.
3. **Allewell, N. M.** 1989. *Escherichia coli* aspartate transcarbamoylase: structure, energetics, and catalytic and regulatory mechanisms. Annu. Rev. Biophys. Biochem. Chem. **18:**71–92.
4. **Beck, D., K. M. Kedzie, and J. R. Wild.** 1989. Comparison of the aspartate transcarbamoylases from *Serratia marcescens* and *Escherichia coli*. J. Biol. Chem. **264:**16629–16637.
5. **Brown, J. W., C. J. Daniels, and J. N. Reeve.** 1989. Gene structure, organization, and expression in archaebacteria. Crit. Rev. Microbiol. **16:**287–338.
6. **Bult, C. J., O. White, G. J. Olsen, L. Zhou, R. D. Fleischmann, G. G. Sutton, J. A. Blake, L. M. FitzGerald, R. A. Clayton, J. D. Gocayne, A. R. Kerlavage, B. A. Dougherty, J. F. Tomb, M. D. Adams, C. I. Reich, R. Overbeek, E. F. Kirkness, K. G. Weinstock, J. M. Merrick, A. Glodek, J. L. Scott, N. S. M. Geoghagen, J. F. Weidman, J. L. Fuhrmann, E. A. Presley, D. Nguyen, T. R. Utterback, J. M. Kelley, J. D. Peterson, P. W. Sadow, M. C. Hanna, M. D. Cotton, M. A. Hurst, K. M. Roberts, B. P. Kaine, M. Borodovsky, H. P. Klenk, C. M. Fraser, H. O. Smith, C. R. Woese, and J. C. Venter.** 1996. Complete genome sequence of the methanogenic archaeon *Methanococcus jannaschii*. Science **273:**1056–1073.
7. **Charbonnier, F., G. Erauso, T. Barbeyron, D. Prieur, and P. Forterre.** 1992. Evidence that a plasmid from a hyperthermophilic archaebacterium is relaxed at physiological temperatures. J. Bacteriol. **174:**6103–6108.
8. **Cohlberg, J. A., V. P. Pigiet, Jr., and H. K. Schachman.** 1972. Structure and arrangement of the regulatory subunits in aspartate transcarbamoylase. Biochemistry **11:**3396–3411.
9. **Cunin, R., M. E. Wales, F. Van Vliet, C. De Staercke, L. Scapozza, C. Swarupa Rani, and J. R. Wild.** 1996. Allosteric regulation in a family of enterobacterial aspartate transcarbamylases: intramolecular transmission of regulatory signals in chimeric enzymes. J. Mol. Biol. **262:**258–269.
10. **Davidson, J. N., K. C. Chen, R. S. Jamison, L. A. Musmanno, and C. B. Kern.** 1993. The evolutionary history of the 1st 3 enzymes in pyrimidine biosynthesis. Bioessays **15:**157–164.
11. **Davidson, J. N., and M. E. Wales.** 1996. Alignment of aspartate transcarbamylase sequences. Paths Pyrimidines **4:**11–17.
12. **De Staercke, C., F. Van Vliet, X. G. Xi, C. Rani, M. Ladjimi, A. Jacobs, F. Triniolles, G. Hervé, and R. Cunin.** 1995. Intramolecular transmission of the ATP regulatory signal in *Escherichia coli* aspartate transcarbamylase: specific involvement of a clustered set of amino acid interactions at an interface between regulatory and catalytic subunits. J. Mol. Biol. **246:**132–143.

12a. **Durbecq, V., et al.** Unpublished data.

13. **England, P., and G. Hervé.** 1992. Synergistic inhibition of *Escherichia coli* aspartate transcarbamylase by CTP and UTP: binding studies using continuous-flow dialysis. Biochemistry **31:**9725–9732.
14. **England, P., C. Leconte, P. Tauc, and G. Hervé.** 1994. Apparent cooperativity for carbamylphosphate in *Escherichia coli* aspartate transcarbamoylase only reflects cooperativity for aspartate. Eur. J. Biochem. **222:**775–780.
15. **Erauso, G., F. Charbonnier, T. Barbeyron, P. Forterre, and D. Prieur.** 1992. Preliminary characterization of a hyperthermophilic archaebacterium with a plasmid, isolated from a North Fiji basin hydrothermal vent. C. R. Acad. Sci. Paris Ser. III Sciences Vie **314:**387–393.
16. **Erauso, G., A. L. Reysenbach, A. Godfroy, J. R. Meunier, B. Crump, F. Partensky, J. A. Baross, V. Marteinsson, G. Barbier, N. R. Pace, and D. Prieur.** 1993. *Pyrococcus abyssi* sp. nov., a new hyperthermophilic archaeon isolated from a deep-sea hydrothermal vent. Arch. Microbiol. **160:**338–349.
17. **Evans, D., K. Bein, H. I. Guy, X. Liu, J. A. Molina, and B. H. Zimmermann.** 1993. CAD gene sequence and the domain structure of the mammalian multifunctional protein CAD. Biochem. Soc. Trans. **21:**186–191.
18. **Faure, M., J. H. Camonis, and M. Jacquet.** 1989. Molecular characterization of a *Dictyostelium discoideum* gene encoding a multifunctional enzyme of the pyrimidine pathway. Eur. J. Biochem. **179:**345–358.
19. **Freund, J. N., W. Zerges, P. Scheld, B. P. Jarry, and W. Vergis.** 1986. Molecular organization of the rudimentary gene of *Drosophila melanogaster*. J. Mol. Biol. **189:**25–36. (Erratum, **191:**727.)
20. **Gaboriaud, C., V. Bissery, T. Benchetrit, and J. P. Mornon.** 1987. Hydrophobic cluster analysis: an efficient new way to compare and analyse amino acid sequences. FEBS Lett. **224:**149–155.
21. **Ganter, C., and A. Plückthun.** 1990. Glycine to alanine substitutions in helices of glyceraldehyde-3-phosphate dehydrogenase: effects on stability. Biochemistry **29:**9395–9402.
22. **Glansdorff, N.** 1965. Topography of cotransducible arginine mutations in *Escherichia coli* K-12. Genetics **51:**167–179.
23. **Gouaux, J. E., and W. N. Lipscomb.** 1988. Three-dimensional structure of carbamoyl phosphate and succinate bound to aspartate carbamoyltransferase. Proc. Natl. Acad. Sci. USA **85:**4205–4208.
24. **Griffin, J. H., J. P. Rosenbusch, K. K. Weber, and E. R. Blout.** 1972. Conformational changes in aspartate transcarbamylase. I. Studies of ligand bind-

ing and of subunit interactions by circular dichroism spectroscopy. J. Biol. Chem. **247:**6482–6490.
25. **Henikoff, S.** 1984. Unidirectional digestion with exonuclease III creates targeted breakpoints for DNA sequencing. Gene **28:**351–359.
26. **Hervé, G.** 1989. Aspartate transcarbamylase from *Escherichia coli*, p. 62–79. *In* G. Hervé (ed.), Allosteric enzymes. CRC Press, Inc., Boca Raton, Fla.
26a. **Hervé, G., et al.** Unpublished data.
27. **Hong, J., W. L. Salo, and P. M. Anderson.** 1995. Nucleotide sequence and tissue-specific expression of the multifunctional protein carbamoyl-phosphate synthetase-aspartate transcarbamoylase-dihydroorotase CAD mRNA in *Squalus acanthias*. J. Biol. Chem. **270:**14130–14139.
28. **Honzatko, R. B., and W. N. Lipscomb.** 1982. Interactions of phosphate ligands with *Escherichia coli* aspartate carbamoyltransferase in the crystalline state. J. Mol. Biol. **160:**265–286.
29. **Honzatko, R. B., J. L. Crawford, H. L. Monaco, J. E. Ladner, B. F. P. Edwards, D. R. Evans, S. G. Warren, D. C. Wiley, R. C. Ladner, and W. N. Lipscomb.** 1982. Crystal and molecular structures of native and CTP-liganded aspartate carbamoyl-transferase in the crystalline state. J. Mol. Biol. **160:**265–286.
30. **Hoover, T. A., W. D. Roof, K. F. Foltermann, G. A. O'Donovan, D. A. Bencini, and J. R. Wild.** 1983. Nucleotide sequence of the structural gene *pyrB* that encodes the catalytic polypeptide of aspartate transcarbamoylase of *Escherichia coli*. Proc. Natl. Acad. Sci. USA **80:**2462–2466.
31. **Hui Bon Hoa, G., G. Hamel, A. Else, G. Weill, and G. Hervé.** 1990. A reactor permitting injection and sampling for steady state studies of enzymatic reactions at high pressure: tests with aspartate transcarbamylase. Anal. Biochem. **187:**258–261.
32. **Kantrowitz, E. R., and W. N. Lipscomb.** 1990. *Escherichia coli* aspartate transcarbamylase: the molecular basis for a concerted allosteric transition. Trends Biochem. Sci. **15:**53–59.
33. **Ke, H., W. N. Lipscomb, Y. Cho, and R. B. Honzatko.** 1988. Complex of *N*-phosphonacetyl-L-aspartate with aspartate carbamoyltransferase from *Escherichia coli*. J. Mol. Biol. **204:**725–747.
34. **Kerbiriou, D., and G. Hervé.** 1972. An aspartate transcarbamylase lacking catalytic subunit interactions. I. Disconnection of homotropic and heterotropic interactions under the influence of 2-thiouracil. J. Mol. Biol. **64:**379–392.
35. **Kosman, R. P., J. E. Gouaux, and W. N. Lipscomb.** 1993. Crystal structure of CTP-ligated T-state aspartate transcarbamoylase at 2.5 angstrom resolution: implications for ATCase mutants and the mechanism of negative cooperativity. Proteins Struct. Funct. Genet. **15:**147–176.
36. **Krause, K. L., K. W. Volz, and W. N. Lipscomb.** 1987. The 2.5 Å structure of aspartate carbamoyltransferase complexed with the bisubstrate analogue *N*-phosphonacetyl-L-aspartate. J. Mol. Biol. **193:**527.
37. **Legrain, C., M. Demarez, N. Glansdorff, and A. Piérard.** 1995. Ammonia-dependent synthesis and metabolic channelling of carbamoyl phosphate in the hyperthermophilic archaeon *Pyrococcus furiosus*. Microbiology **141:**1093–1099.
38. **Lemesle-Varloot, L., B. Henrissat, C. Gaboriaud, V. Bissery, A. Morgat, and J. P. Mornon.** 1990. Hydrophobic cluster analysis: procedures to derive structural and functional information from 2-D-representation of protein sequences. Biochimie **72:**555–574.
39. **Lerner, G. C., and R. L. Switzer.** 1986. Cloning and structure of the *Bacillus subtilis* aspartate transcarbamylase gene *pyrB*. J. Biol. Chem. **261:**11156–11165.
40. **Lipscomb, W. N.** 1994. Aspartate transcarbamylase from *Escherichia coli*: activity and regulation. Adv. Enzymol. Relat. Areas Mol. Biol. **68:**67–151.
41. **Lollier, M., L. Jaquet, T. Nedeva, F. Lacroute, S. Potier, and J. L. Souciet.** 1995. As in Saccharomyces cerevisiae, aspartate transcarbamoylase is assembled on a multifunctional protein including a dihydroorotase-like cryptic domain in *Schizosaccharomyces pombe*. Curr. Genet. **28:**138–149.
42. **Major, J. G., M. E. Wales, J. E. Houghton, J. A. Maley, J. N. Davidson, and J. R. Wild.** 1989. Molecular evolution of enzyme structure: construction of a hybrid hamster/*Escherichia coli* aspartate transcarbamoylase. J. Mol. Evol. **28:**442–450.
43. **Matthews, B. W.** 1993. Structural and genetic analysis of protein stability. Annu. Rev. Biochem. **62:**139–160.
44. **Meighen, E. A., V. Pigiet, and H. K. Schachman.** 1970. Hybridization of native and chemically modified enzymes, III: the catalytic subunits of aspartate transcarbamylase. Proc. Natl. Acad. Sci. USA **67:**234–241.
45. **Messing, J., and J. Vieira.** 1982. A new pair of M13 vectors for selecting either DNA strand of double-digest restriction fragments. Gene **19:**269–276.
46. **Michaels, G., R. A. Kelln, and F. E. Nargang.** 1987. Cloning, nucleotide sequence and expression of the *pyrBI* operon of *Salmonella typhimurium* LT2. Eur. J. Biochem. **166:**55–61.
47. **Nagy, M., M. Le Gouar, S. Potier, J. L. Souciet, and G. Hervé.** 1989. The primary structure of the aspartate transcarbamylase region of the *URA2* gene product in *Saccharomyces cerevisiae*. Features involved in activities and in nuclear localization. J. Biol. Chem. **264:**8366–8374.
48. **Nasr, F., N. Bertauche, M. E. Dufour, M. Minet, and F. Lacroute.** 1994. Heterospecific cloning of *Arabidopsis thaliana* cDNAs by direct complementation of pyrimidine auxotrophic mutants of Saccharomyces cerevisiae. I. Cloning and sequence analysis of two cDNAs catalysing the second, fifth and sixth steps of the *de novo* pyrimidine biosynthesis pathway. Mol. Gen. Genet. **244:**23–32.
49. **Needleman, S. B., and C. D. Wunsch.** 1970. A general method applicable to the search for similarities in the amino acid sequence of two proteins. J. Mol. Biol. **48:**443–453.
50. **Nicholson, H., D. E. Anderson, S. Dao-Pin, and B. W. Matthews.** 1991. Analysis of the interaction between charged side chains and the α-helix dipole using designed thermostable mutants of phage T4 lysozyme. Biochemistry **30:**9816–9828.
51. **Nicholson, H., W. J. Becktel, and B. W. Matthews.** 1988. Enhanced protein thermostability from designed mutations that interact with α-helix dipoles. Nature **336:**651–656.
52. **Norberg, P., J. G. Kaplan, and D. J. Kuschner.** 1973. Kinetics and regulation of the salt-dependent aspartate transcarbamylase of *Halobacterium cutirubrum*. J. Bacteriol. **113:**680–686.
53. **Nowlan, S. F., and E. R. Kantrowitz.** 1985. Superproduction and rapid purification of *Escherichia coli* aspartate transcarbamylase and its catalytic subunit under extreme derepression of the pyrimidine pathway. J. Biol. Chem. **260:**14712–14716.
54. **Overduin, B., S. A. Hogenhout, E. A. Vanderbiezen, M. A. Haring, H. J. J. Nijkamp, and J. Hille.** 1993. The *Asc* locus for resistance to Alternaria stem canker in tomato does not encode the enzyme aspartate carbamoyltransferase. Mol. Gen. Genet. **240:**43–48.
55. **Peitsch, M. C.** 1995. Protein modeling by E-mail. Bio/Technology **13:**658–660.
56. **Peitsch, M. C.** 1996. PpoMod and Swiss-Model: Internet-based tools for automated comparative protein modeling. Biochem. Soc. Trans. **24:**274–279.
57. **Perbal, B., and G. Hervé.** 1972. Biosynthesis of *Escherichia coli* aspartate transcarbamylase. I. Parameters of gene expression and sequential biosynthesis of the subunits. J. Mol. Biol. **70:**511–529.
58. **Purcarea, C.** 1995. Etude des enzymes du métabolisme du carbamylphosphate chez l'archaebacterie marine hyperthermophile et barophile *Pyrococcus abyssi*. Ph.D. thesis. Université Paris-Sud, Paris, France.
59. **Purcarea, C., G. Erauso, D. Prieur, and G. Hervé.** 1994. The catalytic and regulatory properties of aspartate transcarbamoylase from *Pyrococcus abyssi*, a new deep-sea hyperthermophilic archaebacterium. Microbiology **140:**1967–1975.
60. **Richardson, J. S., and D. C. Richardson.** 1988. Amino acid preferences for specific locations at the ends of α helices. Science **240:**1648–1652.
61. **Rost, B., and C. Sander.** 1993. Prediction of protein secondary structure at better than 70% accuracy. J. Mol. Biol. **232:**584–599.
62. **Rost, B., and C. Sander.** 1994. Combining evolutionary information and neutral networks to predict protein secondary structure. Proteins **19:**55–77.
63. **Rost, B., C. Sander, and R. Schneider.** 1994. PHD—a mail server for protein secondary structure prediction. CABIOS **10:**53–60.
64. **Sander, C., and R. Schneider.** 1991. Database of homology-derived structures and the structural meaning of sequence alignement. Proteins **9:**56–68.
65. **Sanger, F., S. Nicklen, and A. R. Coulson.** 1977. DNA sequencing with chain-terminating inhibitors. Proc. Natl. Acad. Sci. USA **74:**5463–5467.
66. **Schachman, H. K., C. D. Pauza, M. Navre, M. J. Karels, L. Wu, and Y. R. Yang.** 1984. Location of amino acid alterations in mutants of aspartate transcarbamoylase: structural aspects of interallelic complementation. Proc. Natl. Acad. Sci. USA **81:**115–119.
67. **Schurr, M. J., J. F. Vickrey, A. P. Kumar, A. L. Campbell, R. Cunin, R. C. Benjamin, M. S. Shanley, and G. A. O'Donovan.** 1995. Aspartate transcarbamoylase genes of *Pseudomonas putida*: requirement for an inactive dihydroorotase for assembly into the dodecameric holoenzyme. J. Bacteriol. **177:**1751–1759.
68. **Simmer, J. P., R. E. Kelly, J. L. Scully, D. R. Grayson, A. G. Rinker, Jr., S. T. Bergh, and D. R. Evans.** 1989. Mammalian aspartate transcarbamylase ATCase: sequence of the ATCase domain and interdomain linker in the CAD multifunctional polypeptide and properties of the isolated domain. Proc. Natl. Acad. Sci. USA **86:**4382–4386.
69. **Souciet, J. L., M. Nagy, M. Le Gouar, F. Lacroute, and S. Potier.** 1989. Organization of the yeast *URA2* gene: identification of a defective dihydroorotase like domain in the multifunctional complex carbamylphosphate synthetase-aspartate transcarbamylase. Gene **79:**59–70.
70. **Stevens, R. C., Y. M. Chook, C. Y. Cho, W. N. Lipscomb, and E. R. Kantrowitz.** 1991. *Escherichia coli* aspartate carbamoyltransferase: the probing of crystal structure analysis via site-specific mutagenesis. Protein Eng. **4:**391–408.
71. **Stevens, R. C., J. E. Gouaux, and W. N. Lipscomb.** 1990. Structural consequences of effector binding to the T-state of aspartate carbamoyltransferase: crystal structures of the unligated and ATP- and CTP-complexed enzymes at 2.6 A resolution. Biochemistry **29:**7691–7701.
72. **Stevens, R. C., and W. N. Lipscomb.** 1992. A molecular mechanism for pyrimidine and purine nucleotide control of aspartate transcarbamoylase. Proc. Natl. Acad. Sci. USA **89:**5281–5285.
73. **Van de Casteele, M.** 1994. The metabolic and genetic control of carbamoylation in extreme thermophilic eubacteria. Ph.D. dissertation. Vrije Universiteit Brussel, Brussels, Belgium.

74. **Van de Casteele, M., M. Demarez, C. Legrain, C. Chen, P. G. Van Lierde, A. Piérard, and N. Glansdorff.** 1994. Genes encoding thermophilic aspartate carbamoyltransferases of *Thermus aquaticus* ZO5 and *Thermotoga maritima* MSB8: modes of expression in *E. coli* and properties of their products. Biocatalysis **11:**165–179.
75. **Van de Casteele, M., M. Demarez, C. Legrain, N. Glansdorff, and A. Piérard.** 1990. Pathways of arginine biosynthesis in extreme thermophilic archaeo- and eubacteria. J. Gen. Microbiol. **136:**1177–1183.
76. **Walker, J. E., A. J. Wonacott, and J. I. Harris.** 1980. Heat stability of a tetrameric enzyme, D-glyceraldehyde-3-phosphate dehydrogenase. Eur. J. Biochem. **108:**581–586.
77. **Wild, J. R., and M. E. Wales.** 1990. Molecular evolution and genetic engineering of protein domains involving aspartate transcarbamoylase. Annu. Rev. Microbiol. **44:**193–218.
78. **Wiley, D. C., and W. N. Lipscomb.** 1968. Crystallographic determination of symmetry of aspartate transcarbamylase. Nature (London) New Biol. **218:** 1119–1121.
79. **Williamson, C. L., and R. D. Slocum.** 1993. Characterization of an aspartate transcarbamoylase cDNA from pea *Pisum sativum* 1. Plant Physiol. **102:** 1055–1056.
80. **Williamson, C. L., and R. D. Slocum.** 1994. Isolation of cDNA clones by complementation of E. coli mutants with infective pBluescript phagemid libraries. BioTechniques **16:**986–987.
81. **Wilson, R., R. Ainscough, K. Anderson, C. Baynes, M. Berks, J. Bonfield, J. Burton, M. Connell, T. Copsey, J. Cooper, A. Coulson, M. Craxton, S. Dear, Z. Du, R. Durbin, A. Favello, L. Fulton, A. Gardner, P. Green, T. Hawkins, L. Hillier, M. Jier, L. Johnston, M. Jones, J. Kershaw, J. Kirsten, N. Laister, P. Latreille, J. Lightning, C. Lloyd, A. McMurray, B. Mortimore, M. O'Callaghan, J. Parsons, C. Percy, L. Rifken, A. Roopra, D. Saunders, R. Shownkeen, N. Smaldon, A. Smith, E. Sonnhammer, R. Staden, J. Sulston, J. Thierry-Mieg, K. Thomas, M. Vaudin, K. Vaughan, R. Waterston, A. Watson, L. Weinstock, J. Wilkinson-Sproat, and P. Wohldman.** 1994. 2.2 Mb of contiguous nucleotide sequence from chromosome III of *C. elegans*. Nature **368:**32–38.
82. **Xi, X. G., C. De Staercke, F. Van Vliet, F. Triniolles, A. Jacobs, P. P. Stas, M. M. Ladjimi, V. Simon, R. Cunin, and G. Hervé.** 1994. The activation of *Escherichia coli* aspartate transcarbamylase by ATP. Specific involvement of helix H2′ at the hydrophobic interface between the two domains of the regulatory chains. J. Mol. Biol. **242:**139–149.
83. **Xi, X. G., F. Van Vliet, M. M. Ladjimi, B. De Wannedmaeker, C. De Staercke, N. Glansdorff, A. Piérard, R. Cunin, and G. Hervé.** 1991. The cooperative interactions between the catalytic sites in *Escherichia coli* aspartate transcarbamylase: role of the C-terminal region of the regulatory chains. J. Mol. Biol. **220:**789–799.
84. **Yutani, K., K. Ogasahara, A. Kimura, and Y. Sugino.** 1982. Effect of single amino acid substitutions at the same position on stability of a two-domain protein. J. Mol. Biol. **160:**387–390.